

2020-04-28

## Electrochemical Performance Improvement of $\text{Li}_2\text{MnO}_3$ Cathode Materials by $\text{MgF}_2$ Coating

Du-dan WANG

Fei WANG

Huan-huan ZHAI

Yu-peng LI

Na-chuan YANG

Kang-hua CHEN

1. *Light Alloy Research Institute, Central South University, Changsha 410083, Hunan, China*; 2. *State Key Laboratory of Powder Metallurgy, Central South University, Changsha 410083, Hunan, China*;  
kanghuachen@csu.edu.cn

---

### Recommended Citation

Du-dan WANG, Fei WANG, Huan-huan ZHAI, Yu-peng LI, Na-chuan YANG, Kang-hua CHEN.  
Electrochemical Performance Improvement of  $\text{Li}_2\text{MnO}_3$  Cathode Materials by  $\text{MgF}_2$  Coating[J]. *Journal of Electrochemistry*, 2020, 26(2): 289-297.  
DOI: 10.13208/j.electrochem.190524  
Available at: <https://jelectrochem.xmu.edu.cn/journal/vol26/iss2/12>

This Article is brought to you for free and open access by Journal of Electrochemistry. It has been accepted for inclusion in Journal of Electrochemistry by an authorized editor of Journal of Electrochemistry.

DOI: 10.13208/j.electrochem.190524

Article ID:1006-3471(2020)02-0289-09

Cite this: *J. Electrochem.* 2020, 26(2): 289-297

Http://electrochem.xmu.edu.cn

## Electrochemical Performance Improvement of $\text{Li}_2\text{MnO}_3$ Cathode Materials by $\text{MgF}_2$ Coating

WANG Du-dan<sup>1</sup>, WANG Fei<sup>2</sup>, ZHAI Huan-huan<sup>1</sup>, LI Yu-peng<sup>2</sup>, YANG Na-chuan<sup>2</sup>, CHEN Kang-hua<sup>1,2\*</sup>

(1. *Light Alloy Research Institute, Central South University, Changsha 410083, Hunan, China;*

2. *State Key Laboratory of Powder Metallurgy, Central South University, Changsha 410083, Hunan, China*)

**Abstract:** Cathode material  $\text{Li}_2\text{MnO}_3$  has received more and more attention owing to its high theoretical capacity ( $459 \text{ mAh} \cdot \text{g}^{-1}$ ). However, the low initial coulombic efficiency and the poor cycle stability hamper its practical application in lithium-ion batteries. Herein, we investigated the crystal structure and electrochemical performance of  $\text{Li}_2\text{MnO}_3$  by introducing  $\text{MgF}_2$  coating layer. The results indicated that the conversion of partial layer  $\text{Li}_2\text{MnO}_3$  to spinel phase induced by  $\text{MgF}_2$  coating could reduce the initial irreversible capacity and improve the first cycle efficiency. The initial coulombic efficiencies of the 0.5wt.%, 1.0wt.%, and 2.0wt.%  $\text{MgF}_2$ -coated electrodes were 70.1%, 77.5% and 84.9%, respectively, compared with 57.7% of the pristine cathode. The charge-discharge curves showed that the 1.0wt.%  $\text{MgF}_2$ -modified  $\text{Li}_2\text{MnO}_3$  delivered the highest charge and discharge capacities, and exhibited the best cycle stability. The capacity retention rate of the 1.0wt.%  $\text{MgF}_2$ -coated sample was 81% after the 40th cycles, which was much higher than that of the pristine sample (53.6%). The electrochemical impedance spectroscopic data revealed that the  $\text{MgF}_2$  coating reduced the rapid deposition of the resistive component and improved the cycle stability of the electrodes.

**Key words:**  $\text{Li}_2\text{MnO}_3$  cathode;  $\text{MgF}_2$  coating; cycle stability; coulombic efficiency

**CLC Number:** O646.21

**Document Code:** A

Lithium-ion batteries have been regarded as the most promising electrochemical energy storage system, and used in electric vehicles and portable electronic devices<sup>[1-3]</sup>. In order to meet the requirement of high energy density, the development of cathode materials with superior electrochemical performance and environmental friendly has become the focus of lithium-ion batteries<sup>[4-7]</sup>. Manganese (Mg)-based lithium (Li)-rich layered compounds as cathode materials are safer, less toxic and cheaper than cobalt (Co) or nickel (Ni)-based layered compounds. Therefore, Mg-based Li-rich layered compounds have received more attention as cathode materials in lithium-ion batteries<sup>[8-11]</sup>. The Mg-based Li-rich layered compound is characterized by an irreversible high voltage platform above 4.5 V during the first charge. This platform is formed by the removal of " $\text{Li}_2\text{O}$ " from  $\text{Li}_2\text{MnO}_3$ <sup>[12-13]</sup>. Mg-based Li-rich layered compounds have high initial discharge capacity owing to the activation of

$\text{Li}_2\text{MnO}_3$ , but the cycle performance is poor. Therefore, it would be beneficial to understand the properties of this type layered compound by re-examination in the properties of the  $\text{Li}_2\text{MnO}_3$  material.

The main problem with  $\text{Li}_2\text{MnO}_3$  is the poor electronic conductivity and the irreversible loss of oxygen, making the structure unstable. Oxygen release during the first charging process results in an irreversible structural change that reduced the coulombic efficiency of the first cycle and accelerated the capacity decay during cycling<sup>[14]</sup>. The common methods of improving  $\text{Li}_2\text{MnO}_3$  performance are surface coating and element doping. Yanhong Xiang<sup>[15]</sup> synthesized the  $\text{Li}_2\text{Mn}_{0.9}\text{Al}_{0.1}\text{O}_3$  compounds. The results showed that the doping of Al could slow the capacity decay and improve the rate performance. However, Loraine Torres-Castro<sup>[16]</sup> used Al instead of the Li site to improve the properties of the  $\text{Li}_2\text{MnO}_3$  material. The data showed that the spinel phase was gradually

formed with the increase of Al content, and the binding energy of the sample was decreased, which improved the electrochemical properties of the material. Toshiyuki Matsunaga<sup>[17]</sup> prepared Ni-doped  $\text{Li}_2\text{MnO}_3$  materials. With the increasing of Ni metal, the number of active Li ions increased, which resulted in high charge and discharge capacities. Lilong Xiong et al. used Na-doped<sup>[18]</sup> or Mg-doped<sup>[19]</sup> Li-site to modify  $\text{Li}_2\text{MnO}_3$  cathode. They deemed that Na or Mg doping could significantly improve the cycle stability and rate performance of the material. In addition, the Mg modification brought the energy density of the  $\text{Li}_2\text{MnO}_3$  material to a new height ( $944 \text{ Wh} \cdot \text{kg}^{-1}$ ) compared with  $747.1 \text{ Wh} \cdot \text{kg}^{-1}$  of  $\text{Li}_2\text{MnO}_3$  without Mg modification. Surface modification can hinder the reaction between electrolyte and electrode, alleviate the rapid growth of the unfavorable solid electrolyte interphase (SEI) film, and improve the electrochemical performance. Hui Liu<sup>[20]</sup> investigated surface-modified  $\text{Li}_{1.2}\text{Ni}_{0.13}\text{Co}_{0.13}\text{Mn}_{0.54}\text{O}_2$  materials with  $\text{NH}_4\text{HF}_2$  coating, indicating that this coating caused chemical precipitation of Li in  $\text{Li}_2\text{MnO}_3$  material. This method effectively enhanced the electrochemical properties of Li-rich Mn-based materials. Yang-Kook Sun<sup>[21]</sup> prepared  $\text{AlF}_3$ -coated  $\text{Li}[\text{Li}_{0.19}\text{Ni}_{0.16}\text{Co}_{0.08}\text{Mn}_{0.57}]\text{O}_2$ . The results indicated that a part of  $\text{Li}_2\text{MnO}_3$  in the material was converted into spinel structure, which effectively improved the electrode rate performance and lithium storage capacity.

Usually,  $\text{MgF}_2$  is stable in the electrolyte of lithium-ion batteries. Here, we report that the improved electrochemical performance of  $\text{Li}_2\text{MnO}_3$  materials by surface modification. In this work,  $\text{Li}_2\text{MnO}_3$  sam-

ples with the surface-coated  $\text{MgF}_2$  were prepared in an attempt to improve the cycle stability. The role of  $\text{MgF}_2$  coating in the electrochemical performance of  $\text{Li}_2\text{MnO}_3$  at room temperature has been investigated.

## 1 Experimental

### 1.1 Reagents and Instruments

The reagents used in this work and their parameters are listed in Tab. 1.

Tab. 1 Main chemical reagents

Reagent	Purity	Manufacturer
$\text{LiCH}_3\text{COO} \cdot 2\text{H}_2\text{O}$	AR	Aladdin
$\text{Mn}(\text{CH}_3\text{COO})_2 \cdot 4\text{H}_2\text{O}$	AR	Aladdin
$\text{MgCl}_2$	AR	Aladdin
$\text{NH}_4\text{F}$	AR	Aladdin
$\text{C}_6\text{H}_8\text{O}_7 \cdot \text{H}_2\text{O}$	AR	Aladdin

The names, models and sources of the equipments involved in this work are listed in Tab. 2.

### 1.2 Experimental Method

The pristine  $\text{Li}_2\text{MnO}_3$  sample was synthesis by solgel method. Stoichiometric amounts of  $\text{LiCH}_3\text{COO} \cdot 2\text{H}_2\text{O}$  and  $\text{Mn}(\text{CH}_3\text{COO})_2 \cdot 4\text{H}_2\text{O}$  were dissolved in deionized water to form metal ions solution. The citric acid solution was added to the above metal ions solution with constant stirring, and then this mixed solution was evaporated at  $80 \text{ }^\circ\text{C}$  to obtain a viscous gel. Next, the gel was dried completely at  $120 \text{ }^\circ\text{C}$  for 10 h. Finally, the resultant precursor was heated to  $500 \text{ }^\circ\text{C}$  for 4 h. To prepare the  $\text{MgF}_2$ -coated  $\text{Li}_2\text{MnO}_3$ ,  $\text{NH}_4\text{F}$  and  $\text{MgCl}_2$  were dissolved in deionized water,

Tab. 2 Main instruments

Name	Model	Factory
Electronic balance	ALC-210.4	ACCULRB sartorius group
Blast drying oven	101	Beijing Guangming Medical Co., Ltd.
Tube furnace	TCW-32B	Yixing Opry Furnace Industry
Magnetic heating stirrer	DF-101S	Zhengzhou Changcheng Branch Industry and Trade Co., Ltd.
LAND test system	CT2001A	Wuhan Landian Electronics Co., Ltd.
Electrochemical workstation	CHI660A	Shanghai Zhenhua Instrument Company

respectively. Afterwards the obtained  $\text{Li}_2\text{MnO}_3$  powder was added in the  $\text{MgCl}_2$  solution, and then the  $\text{NH}_4\text{F}$  solution was added with continuous stirring. The weight ratios of  $\text{MgF}_2$  to  $\text{Li}_2\text{MnO}_3$  powder were 0.5%, 1.0% and 2.0%, respectively. The solution was dried at  $80^\circ\text{C}$  in an oven. The obtained  $\text{MgF}_2$ -coated  $\text{Li}_2\text{MnO}_3$  powder was heated at  $400^\circ\text{C}$  for 3 h in air.

The phase structure was analyzed by X-ray diffraction (XRD) using  $\text{Cu K}_\alpha$  radiation. The scanning range was  $10^\circ \leq 2\theta \leq 80^\circ$  and the scanning rate was  $8^\circ \cdot \text{min}^{-1}$ . Scanning electron microscope (SEM) was used to analyze the morphology and particle size of the samples. Energy-dispersive spectroscope (EDS) was employed in combination with SEM to roughly determine the element content of powder. The active material was mixed with polyvinylidene fluoride and conductive carbon black in a mass ratio of 80:10:10 and stirred with N-methylpyrrolidone to form slurry. The slurry was coated into the Al foil current collector and dried thoroughly at  $80^\circ\text{C}$  in an oven. The CR2032 type cells consisted of Li metal anode and cathode separated by a polypropylene film were assembled in an argon-filled glove box. The electrolyte solution was  $1 \text{ mol} \cdot \text{L}^{-1}$   $\text{LiPF}_6$ -DMC/EC (1:1 by volume) that purchased from DouDou Chemical Company. The charge-discharge measurements were carried out in LAND CT2001A test system in the voltage range from 2.0 to 4.8 V. The data of electrochemical impedance spectroscopy (EIS) was collected on an electrochemical workstation in the frequency range from 100 kHz to 0.1 Hz.

## 2 Results and Discussion

The XRD patterns of the  $\text{MgF}_2$ -coated and pristine  $\text{Li}_2\text{MnO}_3$  materials are shown in Fig. 1. The characteristic peaks of all the samples were basically consistent with the standard lines of the monoclinic layered structure  $\text{Li}_2\text{MnO}_3$  (PDF No. 84-1634, space group  $\text{C2/m}$ ). As can be seen in Fig. 1, the 1.0wt.% and 2.0wt.%  $\text{MgF}_2$ -coated materials had the characteristic peak belonging to spinel structure around  $37^\circ$ , indicating that the  $\text{MgF}_2$  coating induced the transformation of  $\text{Li}_2\text{MnO}_3$  from layered structure to spinel structure. No diffraction peaks associated with  $\text{MgF}_2$

were observed in the  $\text{MgF}_2$ -coated  $\text{Li}_2\text{MnO}_3$  samples, indicating that this coating layer was not presented as a crystalline phase. This might probably be caused by the low heat treating temperature of  $400^\circ\text{C}$ , which is not sufficient for  $\text{MgF}_2$  to form a crystalline coating layer<sup>[22-23]</sup>.

The morphology and particle size of the  $\text{MgF}_2$ -coated and pristine  $\text{Li}_2\text{MnO}_3$  particles are shown in Fig. 2. Evidently, the surface morphology of the  $\text{Li}_2\text{MnO}_3$  particles modified by  $\text{MgF}_2$  was changed. With the increasing amount of  $\text{MgF}_2$ , most of the surfaces were covered by the coating film. The

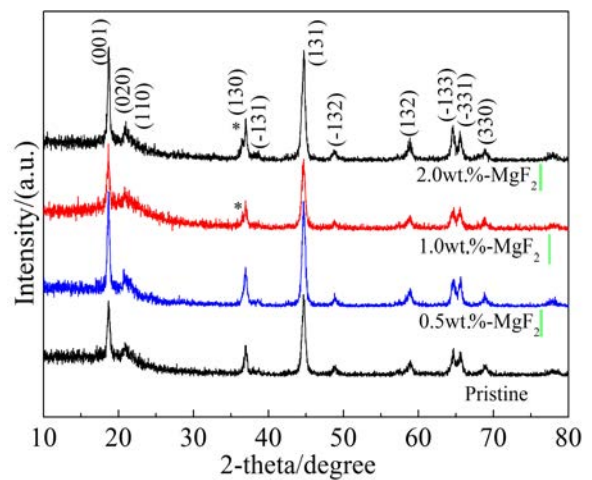


Fig. 1 X-ray diffraction patterns of the pristine and different  $\text{MgF}_2$ -coated  $\text{Li}_2\text{MnO}_3$  samples

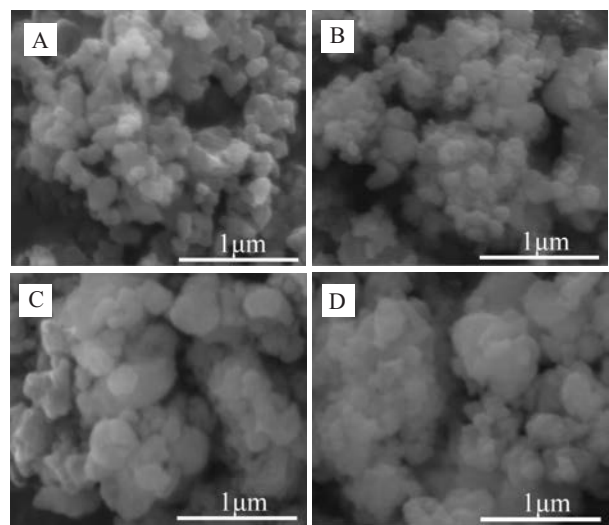


Fig. 2 SEM images of (A) the pristine, (B) 0.5wt.%, (C) 1.0wt.%, and (D) 2.0wt.%  $\text{MgF}_2$ -coated  $\text{Li}_2\text{MnO}_3$  samples

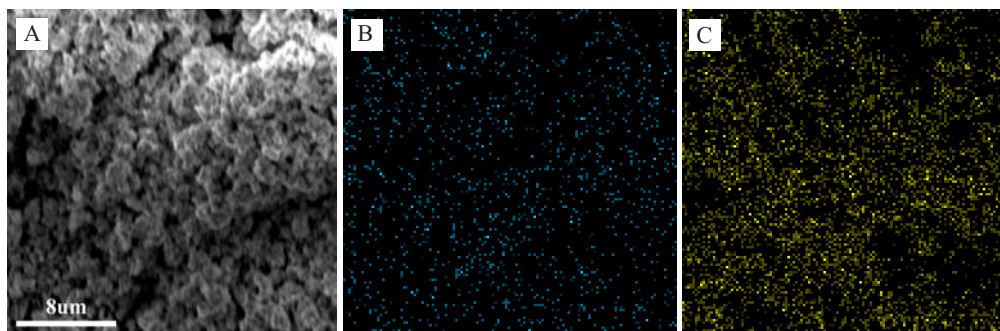


Fig. 3 SEM image (A) and the corresponding EDS mapping images of 1.0wt.%  $\text{MgF}_2$ -coated  $\text{Li}_2\text{MnO}_3$  for (B) Mg and (C) F elements

$\text{MgF}_2$ -coated particles tended to aggregate to form large particles, and the corners and edges became blurred. The  $\text{MgF}_2$  coating could inhibit the contact between the electrolyte and the particles, and prevent the dissolution of  $\text{Mn}^{3+}$ . Fig. 3(B-C) displays the EDS mapping images of 1.0wt.%  $\text{MgF}_2$ -coated sample from Fig. 3(A). It can be seen from Fig. 3(B-C) that Mg and F elements were uniformly distributed in the surface. As shown in Fig. 4, the 1.0wt.%  $\text{MgF}_2$ -coated  $\text{Li}_2\text{MnO}_3$  surface (A) revealed a uniform film compared to the pristine sample surface (B), confirming that the surface of  $\text{Li}_2\text{MnO}_3$  was successfully coated with  $\text{MgF}_2$  film.

Fig. 5(A) exhibits the initial charge-discharge curves of the pristine and  $\text{MgF}_2$ -coated  $\text{Li}_2\text{MnO}_3$  cathodes at 0.1 C ( $20 \text{ mA} \cdot \text{g}^{-1}$ ) rate. Similar to the previously reported  $\text{Li}_2\text{MnO}_3$  electrode, all the samples showed a significant charging platform around 4.5 V, which corresponds to the “ $\text{Li}_2\text{O}$ ” extraction from the  $\text{Li}_2\text{MnO}_3$  lattice structure<sup>[12-13]</sup>. However, the width of

this platform was decreased as the amount of  $\text{MgF}_2$  coating increased, and when the amount of  $\text{MgF}_2$  coating increased to 2.0wt.%, the electrode had a very short voltage platform and capacity was only  $129 \text{ mAh} \cdot \text{g}^{-1}$ . In addition, the modified sample showed a voltage platform at 2.8 V, which is feature of the spinel phase ( $\text{LiMn}_2\text{O}_4$ )<sup>[24-25]</sup>, and the platform became more and more obvious as the amount of  $\text{MgF}_2$  coating increased. It indicates that the  $\text{MgF}_2$  coating induced the transition of the layered structure to the spinel structure, agreed with the XRD data.

The cycle performance curves of the  $\text{MgF}_2$ -coated and pristine  $\text{Li}_2\text{MnO}_3$  cathodes are presented in Fig. 5(B). As we can see from the discharge curve, there was a sequential phase transformation: monoclinic  $\text{C2/m} \rightarrow$  tetragonal  $\text{I41} \rightarrow$  cubic spinel<sup>[26]</sup>. It was clear from Fig. 4(B) that the capacity retention rate of the  $\text{MgF}_2$ -modified electrode was higher than that of the pristine electrode. Capacity retention values were 65% for 0.5wt.%, 81% for 1.0wt.%, and 72.2% for 2.0wt.%  $\text{MgF}_2$ -modified cathodes, compared with 53.6% for the pristine cathode. In addition, owing to the formation of a large number of spinel phases, the discharge capacity tended to be increased and then decreased as the amount of  $\text{MgF}_2$  increased. The reason why the cycle performance of the  $\text{MgF}_2$ -modified electrodes was enhanced is that the spinel structure might be stably circulated<sup>[27]</sup> and the  $\text{MgF}_2$  coating could avoid the contact between the electrolyte and the particles<sup>[28]</sup>.

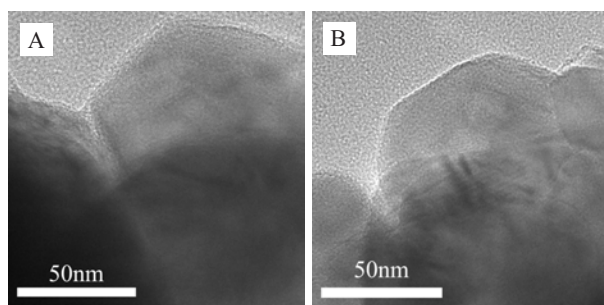


Fig. 4 TEM images of (A) the pristine  $\text{Li}_2\text{MnO}_3$  and (B) 1.0wt.%  $\text{MgF}_2$ -coated  $\text{Li}_2\text{MnO}_3$

Tab. 3 presents the initial capacity and coulom

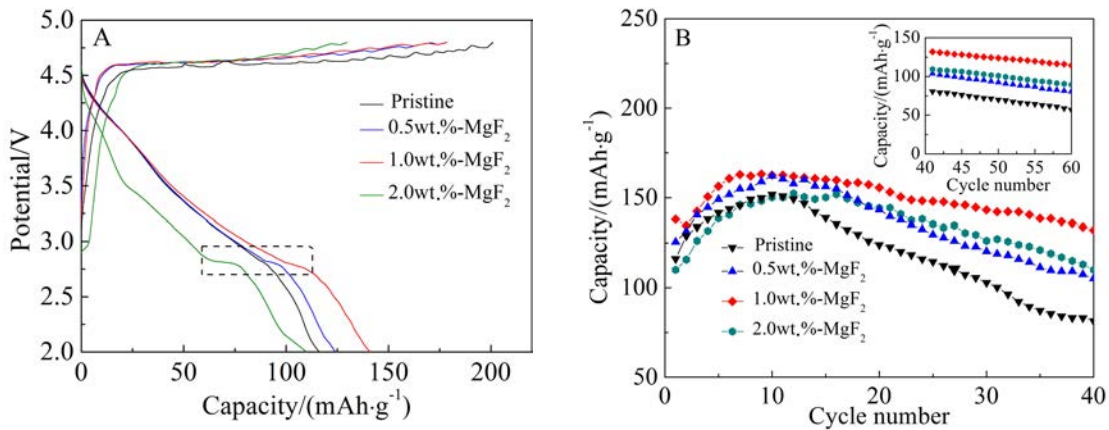


Fig. 5 (A) The initial charge-discharge curves and (B) the cycle performance curves of the pristine and  $\text{MgF}_2$ -coated  $\text{Li}_2\text{MnO}_3$  samples

bic efficiency for the  $\text{MgF}_2$ -coated and pristine  $\text{Li}_2\text{MnO}_3$  electrodes. Compared with the pristine electrode, the 0.5wt.% and 1.0wt.%  $\text{MgF}_2$ -coated electrodes exhibited an increased discharge capacity, that may be owing to the combination of the stabilized electrolyte/cathode interface and partial spinel structure induced by  $\text{MgF}_2$  coating. As the amount of  $\text{MgF}_2$  increased, the first cycle efficiency increased gradually. The first cycle efficiencies of different modified electrodes were higher than that of the pristine electrode. During the first charging period, the “ $\text{Li}_2\text{O}$ ” which was removed from the  $\text{Li}_2\text{MnO}_3$  above 4.5 V could not be re-inserted, resulting in irreversible capacity loss. The conversion of partial  $\text{Li}_2\text{MnO}_3$  induced by  $\text{MgF}_2$  coating to  $\text{LiMn}_2\text{O}_4$  might reduce the initial irreversible capacity and improve the first cycle efficiency.

As shown in Fig. 6, three consecutive cyclic voltammograms of the pristine  $\text{Li}_2\text{MnO}_3$  and

$\text{MgF}_2$ -coated  $\text{Li}_2\text{MnO}_3$  electrodes were obtained at a scanning rate of  $0.1 \text{ mV} \cdot \text{s}^{-1}$ . During the initial charging of the pristine  $\text{Li}_2\text{MnO}_3$  sample, no anodic peak was observed around 4.0 V. However, this characteristic peak of spinel phase ( $\text{LiMn}_2\text{O}_4$ ) appeared in the subsequent cycle with the weak intensity. Contrastly, the characteristic peak of spinel phase was observed at the first cycle as the  $\text{MgF}_2$  amount increased, indicating that this coating could induce a phase transition from layer to spinel<sup>[18,29]</sup>. The oxidation peak around 4.5 V was connected to the removal of “ $\text{Li}_2\text{O}$ ” from the  $\text{Li}_2\text{MnO}_3$  material. Owing to the formation of layered  $\text{LiMnO}_2$  ( $\text{Li} + \text{MnO}_2 \rightarrow \text{LiMnO}_2$ ), a cathodic peak around 3.2 V was observed during the discharging for all the samples<sup>[30]</sup>. A reduction peak at 2.8 V, which is feature of the spinel phase<sup>[20-21]</sup>, was observed, and its intensity gradually became stronger with the increasing  $\text{MgF}_2$  amount, which is consistent with the evolution of the discharge platform.

Tab. 3 Initial charge and discharge capacities, and the first cycle efficiency of the pristine and  $\text{MgF}_2$ -coated  $\text{Li}_2\text{MnO}_3$  electrodes cycled between 2.0 and 4.8 V at a current density of  $20 \text{ mA} \cdot \text{g}^{-1}$

$\text{Li}_2\text{MnO}_3$ sample	Charge capacity/ ( $\text{mAh} \cdot \text{g}^{-1}$ )	Discharge capacity/ ( $\text{mAh} \cdot \text{g}^{-1}$ )	First cycle efficiency/%
Pristine	200.9	116.1	57.7
0.5wt.%- $\text{MgF}_2$	178.2	125.6	70.1
1wt.%- $\text{MgF}_2$	178.5	138.2	77.5
2wt.%- $\text{MgF}_2$	129.7	110	84.9

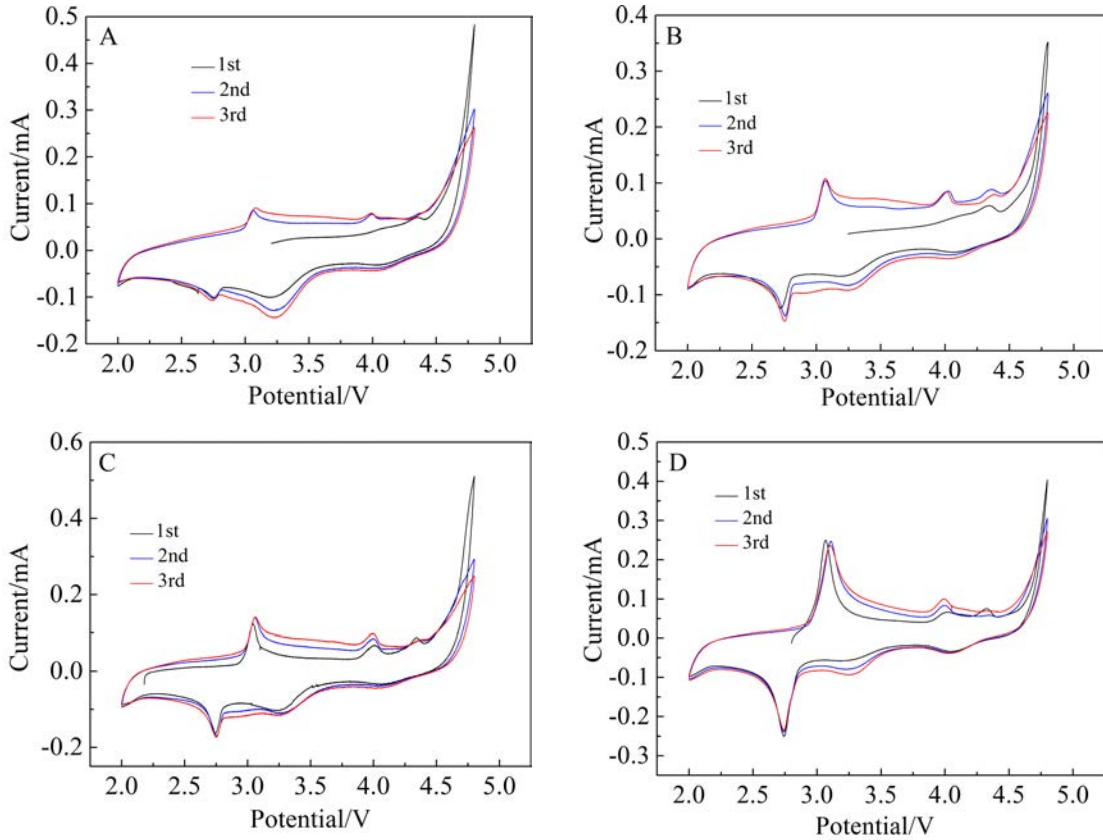


Fig. 6 Cyclic voltammograms of (A)  $\text{Li}_2\text{MnO}_3$ , (B) 0.5wt.% $\text{MgF}_2$ - $\text{Li}_2\text{MnO}_3$ , (C) 1.0wt.% $\text{MgF}_2$ - $\text{Li}_2\text{MnO}_3$  and (D) 2.0wt.% $\text{MgF}_2$ - $\text{Li}_2\text{MnO}_3$  in the voltage range of 2.0 ~ 4.8 V with a scan rate of  $0.1 \text{ mV} \cdot \text{s}^{-1}$

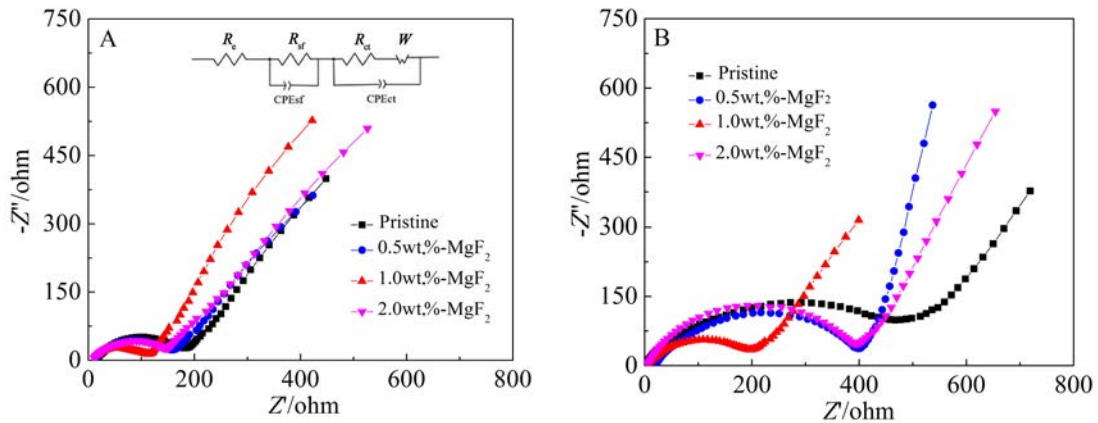


Fig. 7 Nyquist plots of the pristine and  $\text{MgF}_2$ -coated  $\text{Li}_2\text{MnO}_3$  samples: (A) before the cycle and (B) after the 40th cycle

The alternating current (AC) impedance spectra of the  $\text{MgF}_2$ -coated and pristine  $\text{Li}_2\text{MnO}_3$  electrodes, and the equivalent circuit are presented in Fig. 7. In the equivalent circuit (the inset in Fig. 7(A)),  $W$ ,  $R_e$ ,  $R_{ct}$  and  $R_{sf}$  represent the Warburg impedance of lithium ion diffusion, the resistance of liquid electrolyte, charge transfer resistance and electrode surface film

resistance, respectively. The semicircle in the high frequency region of Nyquist plot could elucidate  $R_{sf}$ , and the fitted values are compared in Tab. 4. As we can see from Tab. 4, the  $\text{MgF}_2$ -modified electrodes showed lower  $R_{sf}$  value than the pristine electrode before the cycle. However, the  $R_{sf}$  value of the pristine electrode increased significantly faster than those of

Tab. 4 The fitted  $R_{\text{sf}}$  values of the pristine and  $\text{MgF}_2$ -coated  $\text{Li}_2\text{MnO}_3$  electrodes

$R_{\text{sf}}$	Pristine	0.5wt.-%- $\text{MgF}_2$	1wt.-%- $\text{MgF}_2$	2wt.-%- $\text{MgF}_2$
0	180.8	157.8	108	146
40th	424.9	406.3	195.4	352.2

the  $\text{MgF}_2$ -coated electrodes after the 40th cycles, indicating that  $\text{MgF}_2$  coating could reduce the interface impedance. Since the  $\text{MgF}_2$  coating alleviated the rapid growth of the SEI film<sup>[31-32]</sup>, thereby, enhancing the cycle stability of the modified material.

### 3 Conclusions

The pristine and  $\text{MgF}_2$ -coated  $\text{Li}_2\text{MnO}_3$  electrodes were prepared by the sol-gel method. The results showed that the presence of  $\text{MgF}_2$  coating could induce the partial layer structure of the material to the spinel structure, which improved the initial coulombic efficiency and cycle stability of the  $\text{Li}_2\text{MnO}_3$  material. The capacity retention rate of the 1.0wt.-%  $\text{MgF}_2$ -coated  $\text{Li}_2\text{MnO}_3$  sample reached 81% after the 40th cycles, while that of the pristine  $\text{Li}_2\text{MnO}_3$  sample was only 53.6%. In addition, this coating could prevent the  $\text{Li}_2\text{MnO}_3$  particles from directly contacting the electrolyte, reducing the dissolution of  $\text{Mn}^{3+}$  and the oxidation of the electrolyte. The results presented in this work suggested that the  $\text{MgF}_2$  surface modification might be practically applicable to lithium-rich layered compounds to improve their electrochemical performance.

### Acknowledgements

This work was supported by the National Natural Science Foundation of China (No. 51327902).

### References:

- [1] Croy J R, Abouimrane A, Zhang Z C, et al. Next-generation lithium-ion Batteries: The promise of near-term advancements[J]. MRS Bulletin, 2014, 39(5): 407-415.
- [2] Dunn B, Kamath H, Tarascon J M. Electrical energy storage for the grid: A battery of choices[J]. Science, 2011, 334 (6058): 928-935.
- [3] Goodenough J B. Electrochemical energy storage in a sustainable modern society[J]. Energy & Environmental Science, 2013, 7(1): 14-18.
- [4] Wang J X, Liu Z M, Yan G C, et al. Improving the electrochemical performance of lithium vanadium fluorophosphate cathode material: Focus on interfacial stability[J]. Journal of Power Sources, 2016, 329(5): 553-557.
- [5] Amine K, Kanno R, Tzeng Y H. Rechargeable lithium batteries and beyond: progress, challenges, and future directions[J]. MRS Bulletin, 2014, 39(5): 395-409.
- [6] Tarascon J M, Armand M. Issues and challenges facing rechargeable lithium batteries[J]. Nature, 2001, 414(6861): 359-367.
- [7] Sun Y K, Myung S T, Park B C, et al. High-energy cathode material for long-life and safe lithium batteries[J]. Nature Materials, 2009, 8(4): 320-324.
- [8] The control and performance of  $\text{Li}_4\text{Mn}_5\text{O}_{12}$  and  $\text{Li}_2\text{MnO}_3$  phase ratios in the lithium-rich cathode materials[J]. Electrochimica Acta, 2016, 190: 1142-1149.
- [9] Yan J H, Liu X B, Li B Y. Recent progress in Li-rich layered oxides as cathode materials for Li-ion batteries[J]. RSC Advances, 2014, 4: 63268-63284.
- [10] Zhong S K, Hu P, Luo X, et al. Preparation of  $\text{LiNi}_{0.5}\text{Mn}_{1.5}\text{O}_4$  cathode materials by electrospinning[J]. Ionics, 2016, 22 (11): 2037-2044.
- [11] Wu L, Lu J J, Wei G, et al. Synthesis and electrochemical properties of  $x\text{LiMn}_{0.9}\text{Fe}_{0.1}\text{PO}_4 \cdot y\text{Li}_3\text{V}_2(\text{PO}_4)_3/\text{C}$  composite cathode materials for lithium-ion batteries[J]. Electrochimica Acta, 2014, 146: 288-294.
- [12] Chen H, Islam M S. Lithium extraction mechanism in Li-rich  $\text{Li}_2\text{MnO}_3$  involving oxygen hole formation and dimerization[J]. Chemistry of Materials, 2016, 28(18): 6656-6663.
- [13] Matsunaga T, Komatsu H, Shimoda K, et al. Structural understanding of superior battery properties of partially Ni-doped  $\text{Li}_2\text{MnO}_3$  as cathode material[J]. The Journal of Physical Chemistry Letters, 2016, 7(11): 2063-2067.
- [14] Cho E, Kim K, Jun C, et al. Overview of the oxygen behavior in the degradation of  $\text{Li}_2\text{MnO}_3$  cathode material[J]. The Journal of Physical Chemistry C, 2017, 121 (39): 21118-21127.
- [15] Xiang Y H, Wu X W. Enhanced electrochemical performances of  $\text{Li}_2\text{MnO}_3$  cathode materials by Al doping[J]. Ionics, 2018, 24(1): 83-89
- [16] Torres-Castro L, Shojan J, Julien C M, et al. Synthesis, characterization and electrochemical performance of Al-



- substituted  $\text{Li}_2\text{MnO}_3$ [J]. *Materials Science and Engineering B - Advanced Functional Solid-State Materials*, 2015, 201: 13-22.
- [17] Matsunaga T, Komatsu H, Shimoda K, et al. Structural understanding of superior battery properties of partially Ni-doped  $\text{Li}_2\text{MnO}_3$  as cathode material[J]. *Journal of Physical Chemistry Letters*, 2016, 7(11): 2063-2067.
- [18] Dong X, Xu Y L, Xiong L L, et al. Sodium substitution for partial lithium to significantly enhance the cycling stability of  $\text{Li}_2\text{MnO}_3$  cathode material[J]. *Journal of Power Sources*, 2013, 243: 78-87.
- [19] Zhao W, Xiong L L, Xu Y L, et al. Magnesium substitution to improve the electrochemical performance of layered  $\text{Li}_2\text{MnO}_3$  positive-electrode material[J]. *Journal of Power Sources*, 2016, 330: 37-44.
- [20] Liu H, Du C Y, Yin G P, et al. An Li-rich oxide cathode material with mosaic spinel grain and a surface coating for high performance Li-ion batteries[J]. *Journal of Materials Chemistry A*, 2014, 2(37): 15640-15646.
- [21] Sun Y K, Lee M J, Yoon C S, et al. The role of  $\text{AlF}_3$  coatings in improving electrochemical cycling of Li-enriched nickel-manganese oxide electrodes for Li-ion batteries[J]. *Advanced Materials*, 2012, 24(9): 1192-1196.
- [22] Myung S T, Izumi K, Komaba S, et al. Role of alumina coating on Li-Ni-Co-Mn-O particles as positive electrode material for lithium-ion batteries[J]. *Chemistry of Materials*, 2005, 17(14): 3695-3704.
- [23] Park J H, Yoon S J, Lee H Y, et al. Estimating the burden of psychiatric disorder in Korea[J]. *Journal of Preventive Medicine and Public Health*, 2006, 39(1): 39-45.
- [24] Thackeray M M, Kock A D, Rossouw M H, et al. Spinel electrodes from the Li-Mn-O system for rechargeable lithium battery applications[J]. *Journal of The Electrochemical Society*, 1992, 139(2): 363-366.
- [25] Sun Y K, Jeon Y S, Lee H K. Overcoming Jahn-Teller distortion for spinel Mn phase[J]. *Electrochemical and Solid-State Letters*, 2000, 3(1): 7-9.
- [26] Yan P F, Xiao L, Zheng J M, et al. Probing the degradation mechanism of  $\text{Li}_2\text{MnO}_3$  cathode for Li-ion batteries [J]. *Chemistry of Materials*, 2015, 27(3): 975-982.
- [27] Park S H, Myung S T, Oh S W, et al. Ultrasonic spray pyrolysis of nano crystalline spinel  $\text{LiMn}_2\text{O}_4$  showing good cycling performance in the 3 V range[J]. *Electrochimica Acta*, 2006, 51(19): 4089-4095.
- [28] Bai Y, Jiang K, Sun S W, et al. Performance improvement of  $\text{LiCoO}_2$  by  $\text{MgF}_2$  surface modification and mechanism exploration[J]. *Electrochimica Acta*, 2014, 134: 347-354.
- [29] Yu D Y W, Yanagida K, Kato Y, et al. Electrochemical activities in  $\text{Li}_2\text{MnO}_3$ [J]. *Journal of The Electrochemical Society*, 2009, 156(6): A417-A424.
- [30] Croy J R, Kim D, Balasubramanian M, et al. Countering the voltage decay in high capacity  $x\text{Li}_2\text{MnO}_3 \cdot (1-x)\text{LiMO}_2$  electrodes (M = Mn, Ni, Co) for Li<sup>+</sup>-ion batteries[J]. *Journal of The Electrochemical Society*, 2012, 159(6): A781-A790.
- [31] Wang Q Y, Liu J, Murugan A V, et al. High capacity double-layer surface modified Li [ $\text{Li}_{0.2}\text{Mn}_{0.54}\text{Ni}_{0.13}\text{Co}_{0.13}$ ] $\text{O}_2$  cathode with improved rate capability[J]. *Journal of Materials Chemistry*, 2009, 19(28): 4965-4972.
- [32] Liu J, Manthiram A. Functional surface modifications of a high capacity layered Li [ $\text{Li}_{0.2}\text{Mn}_{0.54}\text{Ni}_{0.13}\text{Co}_{0.13}$ ] $\text{O}_2$  cathode [J]. *Journal of Materials Chemistry*, 2010, 20(19): 3961-3967.

# 富锂层状正极材料 $\text{Li}_2\text{MnO}_3$ 的表面改性及其电化学性能研究

王牡丹<sup>1</sup>, 王非<sup>2</sup>, 翟欢欢<sup>1</sup>, 李玉鹏<sup>2</sup>, 杨纳川<sup>2</sup>, 陈康华<sup>1,2\*</sup>

(1. 中南大学轻合金研究院, 湖南长沙 410083; 2. 中南大学粉末冶金研究院, 湖南长沙 410083)

**摘要:**  $\text{Li}_2\text{MnO}_3$  正极材料具有较高的理论容量 ( $459 \text{ mAh}\cdot\text{g}^{-1}$ ), 不仅安全无毒还能够大大降低电池的制造成本, 从而受到越来越多的关注. 然而, 较低的首圈库仑效率和较差的循环性能妨碍了其在锂电池中的实际应用. 在此, 作者研究了  $\text{MgF}_2$  涂层对  $\text{Li}_2\text{MnO}_3$  正极材料的电化学性能. 结果表明,  $\text{MgF}_2$  涂层诱导部分层状  $\text{Li}_2\text{MnO}_3$  向尖晶石相转化, 从而降低了首圈不可逆容量, 提高库仑效率. 重量比为 0.5%、1.0% 和 2.0% 的  $\text{MgF}_2$  涂层电极的初始库仑效率分别为 70.1%、77.5% 和 84.9%, 而原始电极仅为 57.7%. 充放电曲线表明, 1.0wt.%  $\text{MgF}_2$  涂层改性的  $\text{Li}_2\text{MnO}_3$  具有最高的充放电容量和最佳的循环稳定性. 40 个循环后 1.0wt.%  $\text{MgF}_2$  涂层样品的容量保持率为 81%, 远高于原始样品的容量保持率 (53.6%). 电化学阻抗谱结果表明  $\text{MgF}_2$  涂层减少了不利成分的快速沉积, 并改善了电极的循环稳定性.

**关键词:**  $\text{Li}_2\text{MnO}_3$  正极材料; 氟化镁涂层; 循环稳定性; 库仑效率